

Original Research Article

CircPDSS1 accelerates malignant progression of renal cell carcinoma through sponging of miR-182-5p

Jia Wang¹, Yan Li², Yangsong Ou³, Wan Qin⁴, Wukui Huang⁵, Cengceng Lu⁶, Rongyan Ma⁶, Rui Han², Hu Han^{6*}

¹Department of Nephrology, Ningbo Cilin Hospital, Ningbo, ²Medical Department, The First Affiliated Hospital, School of Medicine, ³Urology Surgery, The First Affiliated Hospital, School of Medicine, Shihezi University, Shihezi, ⁴Department of Oncology, Tongji Hospital, Huazhong University of Science and Technology, Wuhan, ⁵Department of Interventional Diagnosis and Treatment, Affiliated Cancer Hospital, Xinjiang Medical University, Urumqi, ⁶Department of Oncology, The First Affiliated Hospital, School of Medicine, Shihezi University, Shihezi, China

*For correspondence: **Email:** hanhu2022@shzu.edu.cn; **Tel:** +86-18139266163

Sent for review: 6 April 2023

Revised accepted: 3 October 2023

Abstract

Purpose: To investigate the biological function and mechanisms of circPDSS1 in triggering malignant progression of renal cell carcinoma (RCC).

Methods: Quantitative real-time polymerase chain reaction (qRT-PCR) was conducted to determine circPDSS1 levels in 50 pairs of RCC and para-cancerous tissues. The relationship between circPDSS1 level and pathological indices in RCC patients was analyzed, while the *in vitro* effect of circPDSS1 in regulating RCC proliferation was assessed using cell counting kit-8 (CCK-8), colony formation and 5-ethynyl-2'-deoxyuridine (EdU) assay. The sponge effect of circPDSS1 on miR-182-5p was examined by bioinformatics analysis and dual-luciferase reporter assay, while their involvement in mediating malignant progression of RCC was analyzed using rescue experiments. *In vivo*, the influence of circPDSS1 on RCC growth was determined by establishing a xenograft model in nude mice. Thereafter, RCC tissues were harvested from mice to assess relative levels of miR-182-5p and Ki-67.

Results: CircPDSS1 was highly expressed in RCC tissues ($p < 0.05$). A high level of circPDSS1 correlated with advanced tumor staging and low overall survival. Knockdown of circPDSS1 inhibited RCC cell proliferation, and CircPDSS1 sponged and negatively regulated miR-182-5p ($p < 0.05$). MiR-182-5p was able to abolish regulatory effect of circPDSS1 on malignant proliferative potential in RCC cells. *In nude mice bearing RCC, in vivo* knockdown of circPDSS1 slowed down tumor growth and decreased positive expression of Ki-67 in tumor tissues ($p < 0.05$).

Conclusion: CircPDSS1 predicts tumor stage and prognosis in RCC patients. It triggers malignant progression of RCC through sponging of miR-182-5p.

Keywords: CircPDSS1, miR-182-5p, Renal cell carcinoma (RCC), Proliferation

This is an Open Access article that uses a funding model which does not charge readers or their institutions for access and distributed under the terms of the Creative Commons Attribution License (<http://creativecommons.org/licenses/by/4.0>) and the Budapest Open Access Initiative (<http://www.budapestopenaccessinitiative.org/read>), which permit unrestricted use, distribution, and reproduction in any medium, provided the original work is properly credited.

Tropical Journal of Pharmaceutical Research is indexed by Science Citation Index (SciSearch), Scopus, Web of Science, Chemical Abstracts, Embase, Index Copernicus, EBSCO, African Index Medicus, JournalSeek, Journal Citation Reports/Science Edition, Directory of Open Access Journals (DOAJ), African Journal Online, Bioline International, Open-J-Gate and Pharmacy Abstracts

INTRODUCTION

Renal cancer, also known as renal cell carcinoma (RCC), is a malignant tumor derived from renal tubular epithelial cells. Renal cancer

accounts for 85 - 90 % of renal malignant tumors, with 2 - 3 % incidence in adults [1,2]. In China, incidence of RCC shows an upward trend and younger onset [3,4]. Recent onset of RCC in Europe reaches 20,000 cases per year and

about 30,000 in the United States. RCC seriously endangers human health [1-3], and radical resection is usually preferred by RCC patients. Clinical experience has shown that RCC patients poorly respond to chemotherapy and radiotherapy, and the therapeutic efficacy of immune therapy remains uncertain. Therefore, diagnosis of RCC in the early stage and timely surgery are of significance [5,6]. Biological hallmarks that contribute to the diagnosis, treatment and monitoring of RCC are urgently required [7,8]. Experimental research on RCC triggers the emergence of drug-target therapy [9,10]. Identification of specifically expressed genes during the progression of RCC may guide novel treatment in clinical practice [11]. CircRNAs are endogenous RNAs reversely spliced through gene transcription and post-transcriptional regulation, thus participating in cell physiology and disease processes [12,13]. They were initially discovered in viruses and considered to be produced by wrong splicing of gene sequences [13,14]. With the development of high-throughput sequencing and bioinformatics analyses, a great number of circRNAs have been identified in bacteria, plants and animals [14,15]. Some circRNAs are able to translate proteins [16,17]. Importantly, circRNAs are featured by tissue and cell specificities [13-15]. It is believed that circRNAs serve as prognostic and therapeutic hallmarks for tumor diseases [18,19]. Previous studies have shown that circPDSS1 regulates tumor signal transduction in many types of tumor cells [20,21]. This study investigates the role of circPDSS1 in regulating RCC proliferation through *in vitro* experiments and *in vivo* xenograft models in nude mice.

METHOD

RCC samples

Tumor tissues and para-cancerous ones were excised from 50 RCC patients, and stored at -80 °C. Pathological indices were completely recorded. None of the recruited patients received preoperative anti-cancer treatment. This study got ethical approval from the Committee of The First Affiliated Hospital, School of Medicine, Shihezi University (Ethics No. CN-XJ-IRB-72) and it was conducted by following the guidelines in the declaration of Helsinki and Informed consent of each subject was obtained [22].

Cell culture

Human RCC cell lines (ACHN, Caki-1, 769P, Caki-2, 786-O) and renal tubular epithelial cell line (HK-2) were purchased from American Type

Culture Collection (ATCC) (Manassas, VA, USA). The cells were cultured in Dulbecco's Modified Eagle Medium (DMEM) (Gibco, Rockville, MD, USA) in a 5 % CO₂ incubator at 37 °C. The culture medium contained 10 % fetal bovine serum (FBS) (Gibco, Rockville, MD, USA), as well as 100 U/mL penicillin and 100 µg/mL streptomycin.

Transfection

Transfection plasmids were constructed by GenePharma (Shanghai, China). The cells were cultured to 30 - 50 % confluence in 6-well plates and transfected with plasmids using Lipofectamine 2000 (Invitrogen, Carlsbad, CA, USA). After 48 h, cells were collected for transfection efficacy and functional experiments.

Cell proliferation assay

Cells were inoculated in a 96-well plate with 2×10^3 cells per well. Thereafter, the absorbance value at 490 nm of each sample was recorded using cell counting kit-8 (CCK-8) kit (RIBOBIO, Guangzhou, China) for plotting viability curves.

Colony formation assay

Cells were inoculated in a 6-well plate with 200 cells per well and cultured for 2 weeks. The culture medium was replaced once in the first week and twice in the second week. Visible colonies were washed in phosphate-buffered saline (PBS), fixed in methanol for 20 min and dyed in 0.1 % crystal violet for 20 min, and were finally captured and calculated.

5-Ethynyl-2'-deoxyuridine (EdU) assay

The cells were pre-inoculated in a 24-well plate (2×10^4 cells/well). They were incubated in 4 % methanol for 30 min, followed by 10-min permeabilization in 0.5 % TritonX-100 (Solarbio, Beijing, China), and 30-min reaction in 400 µL of 1 × ApollorR. The cells were dyed in 4',6-diamidino-2-phenylindole (DAPI) for another 30 min. Positive EdU-stained cells were counted for calculating EdU-positive rate (Sigma-Aldrich, St. Louis, MO, USA).

Quantitative real-time polymerase chain reaction (qRT-PCR)

Extracted RNAs by TRIzol reagent (Invitrogen, Carlsbad, CA, USA) were purified by DNase I treatment and reversely transcribed into complementary deoxyribose nucleic acids (cDNAs) using Primescript RT Reagent (TaKaRa, Otsu, Japan). The obtained cDNAs

Table 1: Primer sequences

| Gene | | Primer sequences |
|------------|---------|--------------------------------|
| CircPDSS1 | Forward | 5'-GTGGTGCATGAGATCGCCT-3' |
| | Reverse | 5'-GGGTTGTGTGATGAAACCTG-3' |
| GAPDH | Forward | 5'-GAAGGTGAAGGTCGGAGTCGAPD-3' |
| | Reverse | 5'-GAAGATGGTGTGATGGGATTT-3' |
| miR-182-5p | Forward | 5'-TTTGGCAATGGTAGAACTCACACT-3' |
| | Reverse | 5'-GCGAGCACAGAATTAATACGAC-3' |
| U6 | Forward | 5'-CTCGCTTCGGCAGCACACA-3' |
| | Reverse | 5'-AACGCTTCACGAATTTGCGT-3' |

underwent qRT-PCR using SYBR®Premix Ex Taq™ (TaKaRa, Otsu, Japan). Each sample was performed in triplicate. The relative level was calculated using $2^{-\Delta\Delta C_t}$ and normalized to that of glyceraldehyde 3-phosphate dehydrogenase (GAPDH) or U6. The primer sequences are shown in Table 1.

Dual-luciferase reporter assay

HEK293T cells were inoculated in 24-well plates. They were co-transfected with NC mimic/miR-182-5p mimic and circPDSS1-WT/circPDSS1-MUT for 48 h. Cells were lysed and subjected to measurement of luciferase activity (Promega, Madison, WI, USA).

In vivo xenograft model

In vivo xenograft model was established after approval of the Animal Ethics of Shihezi University Animal Center. A total of 10 male nude mice, 8 weeks old were randomly assigned to two groups (n = 5). They were subcutaneously administrated with ACHN cells transfected with sh-NC or sh-circPDSS1, respectively. Tumor size was weekly recorded at a certain time point. Tumor tissues were collected and weighed after sacrificing the mice in the sixth week. Tumor volume (Tv) was calculated using Eq 1.

$$Tv = (W^2L)/2 \dots\dots\dots (1)$$

Where W is the width and L is the length of tumor

Immunohistochemistry (IHC)

Immunohistochemistry was conducted using the streptavidin-peroxidase (SP) method. Positive expression of Ki-67 in RCC sections was determined based on staining color (unstained indicated negative, light yellow indicated weak positive (w), brown indicated positive (p), tan indicated strong positive (sp). The positive rate (Pr) was calculated using Eq 2.

$$Pr = \{(w+p+sp)/N\}100 \dots\dots\dots (2)$$

where N is the total number of cases.

Statistical analysis

Data were expressed as mean \pm standard deviation (SD) and analyzed by Statistical Product and Service Solutions (SPSS) 22.0 (IBM, Armonk, NY, USA). Differences among groups were analyzed using *t*-test. Chi-square analysis was conducted to analyze relationship between circPDSS1 level and pathological indices in RCC patients. The Pearson correlation test was applied to evaluate relationship between relative expressions of two genes. Kaplan-Meier curves were depicted for survival analysis in RCC patients. $P < 0.05$ was considered statistically significant.

RESULTS

Upregulation of circPDSS1 in RCC tissues and cell lines

Compared with para-cancerous tissues, circPDSS1 was upregulated in RCC tissues (Figure 1 A). As expected, higher abundance of circPDSS1 was observed in T3-T4 RCC patients than in T1-T2 patients (Figure 1 B). It was identically upregulated in RCC cell lines (Figure 1 C). Based on the median level of circPDSS1 in RCC tissues, those patients were divided into two groups. CircPDSS1 level was positively linked to tumor staging, whereas it was unrelated to other pathological indices in RCC patients (Table 2).

Knockdown of circPDSS1 inhibited RCC cell proliferation

Human renal adenocarcinoma cells (ACHN) and Caki-2 cells expressed the highest level of circPDSS1 in five tested RCC cell lines. CircPDSS1 knockdown model was established in

two cell lines by transfection of sh-circPDSS1 (Figure 2 A). Compared with those transfected with sh-NC, ACHN and Caki-2 cells transfected with sh-circPDSS1 presented lower viability (Figure 2 B). Reduced colony number and EdU-positive rate in RCC cells with circPDSS1 knockdown further revealed that circPDSS1 triggered proliferative potential in RCC (Figures 2 C and D).

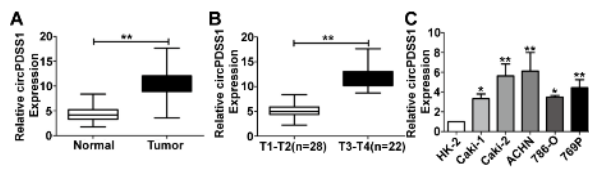


Figure 1: Upregulation of circPDSS1 in RCC tissues and cell lines. (A) Differential expression of circPDSS1 in RCC tissues and paracancerous tissues $**p < 0.01$ vs Normal. (B) CircPDSS1 level in T1-T2 or T3-T4 RCC patients $**p < 0.01$ vs T1-T2. (C) CircPDSS1 level in RCC cell lines $*p < 0.05$, $**p < 0.01$ vs HK-2

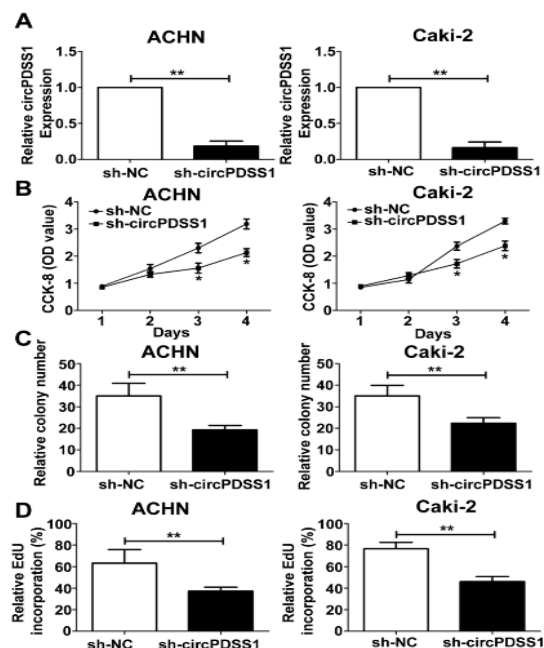


Figure 2: Knockdown of circPDSS1 inhibited RCC cell proliferation. (A) CircPDSS1 levels in ACHN and Caki-2 cells transfected with sh-NC or sh-circPDSS1. (B) Viability of in ACHN and Caki-2 cells transfected with sh-NC or sh-circPDSS1 at days 1, 2, 3 and 4. (C) Relative colony number in ACHN and Caki-2 cells transfected with sh-NC or sh-circPDSS1. (D) EdU-positive rates in ACHN and Caki-2 cells transfected with sh-NC or sh-circPDSS1. $*P < 0.05$, $**p < 0.01$ vs sh-NC

CircPDSS1 was bound to miR-182-5p

Binding relationship between circPDSS1 and miR-182-5p was predicted on three online bioinformatics databases (Figure 3 A). Interestingly, miR-182-5p was upregulated after

knockdown of circPDSS1 in ACHN and Caki-2 cells (Figure 3 B). Conversely, to upregulated trend of circPDSS1, miR-182-5p was downregulated in RCC cell lines and tissues (Figures 3 C and D). Furthermore, the level of MiR-182-5p displayed a negative correlation to circPDSS1 level in RCC tissues (Figure 3 E). Overexpression of miR-182-5p decreased only luciferase activity in the wild-type circPDSS1 vector, confirming the binding between circPDSS1 and miR-182-5p (Figure 3 E).

Table 2: Association of circPDSS1 expression with clinicopathologic characteristics of renal cell cancer

| Parameter | Number of cases | circPDSS1 expression | | P-value |
|-----------------------|-----------------|----------------------|------|---------|
| | | Low | High | |
| Age (years) | | | | 0.812 |
| < 60 | 20 | 12 | 8 | |
| ≥ 60 | 30 | 19 | 11 | |
| Gender | | | | 0.514 |
| Male | 24 | 16 | 8 | |
| Female | 26 | 15 | 11 | |
| T stage | | | | 0.006 |
| T1-T2 | 28 | 22 | 6 | |
| T3-T4 | 22 | 9 | 13 | |
| Lymph node metastasis | | | | 0.190 |
| No | 32 | 22 | 10 | |
| Yes | 18 | 9 | 9 | |
| Distant metastasis | | | | 0.144 |
| No | 35 | 24 | 11 | |
| Yes | 15 | 7 | 8 | |

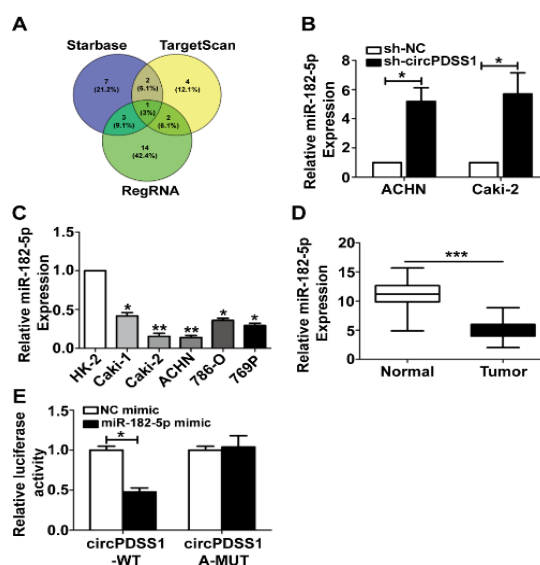


Figure 3: CircPDSS1 was bound to miR-182-5p. (A) Venn diagram on predicted targets of circPDSS1 in three databases. (B) MiR-182-5p level in ACHN and Caki-2 cells transfected with sh-NC or sh-circPDSS1 $*p < 0.05$ vs sh-NC. (C) MiR-182-5p level in RCC cell lines $*p < 0.05$, $**p < 0.01$ vs HK-2. (D) Differential expression of miR-182-5p in RCC tissues and paracancerous tissues $***p < 0.001$ vs Normal. (E)

Luciferase activity in HEK293T cells co-transfected with NC mimic/miR-182-5p mimic and circPDSS1-WT/circPDSS1-MUT. * $P < 0.05$ vs NC mimic

CircPDSS1 exerted a sponging effect on miR-182-5p

Rescue experiments were conducted to investigate the involvement of miR-182-5p in circPDSS1-induced phenotype regulation on RCC. Transfection efficacy of miR-182-5p inhibitor was tested at first (Figure 4 A). Silence of miR-182-5p downregulated increased level of miR-182-5p owing to knockdown of circPDSS1 in RCC cells. Notably, inhibited viability and EdU-positive rate in ACHN and Caki-2 cells with circPDSS1 knockdown were reversed by co-silence of circPDSS1 and miR-182-5p (Figures 4 B and C).

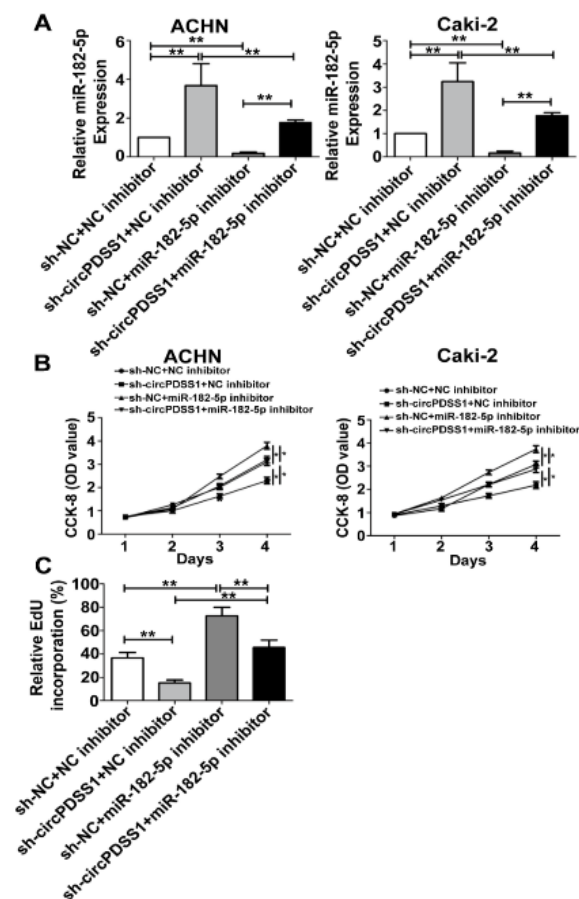


Figure 4: CircPDSS1 exerted a sponging effect on miR-182-5p. (A) MiR-182-5p level in ACHN and Caki-2 cells co-transfected with sh-NC+NC inhibitor, sh-circPDSS1+NC inhibitor, sh-NC+miR-182-5p inhibitor or sh-circPDSS1+miR-182-5p inhibitor. (B) Viability in ACHN and Caki-2 cells co-transfected with sh-NC+NC inhibitor, sh-circPDSS1+NC inhibitor, sh-NC+miR-182-5p inhibitor or sh-circPDSS1+miR-182-5p inhibitor at days 1, 2, 3 and 4. (C) EdU-positive rate in ACHN and Caki-2 cells co-transfected with sh-NC+NC inhibitor, sh-circPDSS1+NC inhibitor, sh-NC+miR-182-5p

inhibitor or sh-circPDSS1+miR-182-5p inhibitor. * $P < 0.05$, ** $p < 0.01$ vs sh-NC+NC inhibitor

Knockdown of circPDSS1 slowed down *in vivo* growth of RCC

Nude mice were administered with ACHN cells transfected with sh-NC or sh-circPDSS1, respectively. Mice were sacrificed to collect RCC tissues after the termination of animal procedures. Lower tumor volume and tumor weight in mice with *in vivo* knockdown of circPDSS1 suggested suppressed RCC growth (Figures 5 A and B). Compared with control, miR-182-5p was up-regulated in RCC tissues harvested from mice with *in vivo* knockdown of circPDSS1 (Figure 5 C). Lower positive expression of Ki-67 was revealed via IHC in RCC tissues with silenced circPDSS1, indicating that circPDSS1 stimulated tumor cell proliferation in nude mice bearing RCC (Figure 5 D).

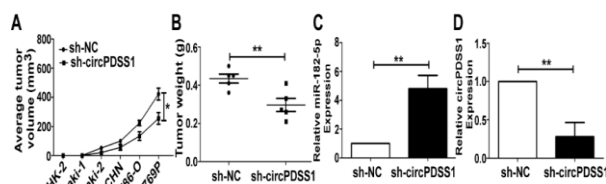


Figure 5: Knockdown of circPDSS1 slowed down *in vivo* growth of RCC. (A) Average tumor volume in nude mice administered with ACHN cells transfected with sh-NC or sh-circPDSS1. (B) Tumor weight in nude mice administrated with ACHN cells transfected with sh-NC or sh-circPDSS1. (C) MiR-182-5p level in RCC tissues collected from nude mice administrated with ACHN cells transfected with sh-NC or sh-circPDSS1. (D) Positive expression of Ki-67 in RCC tissues collected from nude mice administrated with ACHN cells transfected with sh-NC or sh-circPDSS1. * $P < 0.05$, ** $p < 0.01$ vs sh-NC

DISCUSSION

Renal cell carcinoma (RCC) derives from renal tubular epithelial cells, which is responsible for over 90 % of cases of adult renal malignant tumors [4,5]. Histological subtypes of RCC comprise clear cell, papillary, chromophobic and collecting duct, of which, clear cell subtype is the most major one (60 - 85 %) [5,6]. Renal cell carcinoma is the 12th and 17th most common cancer in males and females, respectively [1-4]. It is generally considered that lifestyle-related factors are the greatest risks for RCC [5-7]. In addition, TNM staging, incidental carcinoma, radical resection and postoperative immune therapy largely influence the prognosis in RCC [5-8]. Molecular mechanisms of RCC have been highlighted recently [9-11]. Recently discovered

biomolecules, circRNAs, offer a promising application in gene therapy for tumors [16-18].

CircRNAs present a structure of a covalently closed loop by joining the 5' and 3' terminals [12,13]. As ceRNAs, circRNAs exert an interactive relationship with miRNAs, lncRNAs and proteins [15-17], due to their specificity, stability and abundance, circRNAs are utilized as biological hallmarks [18,19]. It has been reported that circPDSS1 sequences are enriched with miRNA binding sites [20,21]. Differential expressions of circPDSS1 were detected in 50 pairs of RCC tissues, and it was found that circPDSS1 was upregulated in RCC tissues, and its high level indicated advanced tumor staging. It was thus hypothesized that circPDSS1 promotes tumor growth in RCC. Experimental results demonstrated that circPDSS1 triggered proliferative potential in RCC cells. Besides, increased positive expression of Ki-67 in RCC tissues collected from nude mice overexpressing circPDSS1 also supported the *in vitro* findings.

According to bioinformatics tool prediction, circPDSS1 form base complementary pairs with miR-182-5p 3'UTR. Experimental results further validated this prediction. MiR-182-5p was lowly expressed in RCC tissues and cell lines, and it displayed a negative correlation to circPDSS1 level. Furthermore, regulatory effect of circPDSS1 on RCC cell proliferation was abolished by miR-182-5p. Collectively, a negative feedback loop involving circPDSS1/miR-182-5p axis has been identified as a causative factor behind the malignant progression of RCC.

CONCLUSION

The findings of this study suggest that circPDSS1 is a promising biomarker for predicting tumor stage and prognosis in renal cell carcinoma (RCC) patients. Furthermore, understanding the mechanism by which circPDSS1 promotes RCC progression through its interaction with miR-182-5p opens up the possibility of developing targeted therapies that aim to disrupt this interaction, potentially offering a novel therapeutic strategy for RCC treatment in the future. These insights may ultimately contribute to more effective clinical management of RCC and improve patient outcomes.

DECLARATIONS

Acknowledgements

None provided.

Funding

None provided.

Ethical approval

None provided.

Availability of data and materials

The datasets used and/or analyzed during the current study are available from the corresponding author on reasonable request.

Conflict of Interest

No conflict of interest associated with this work.

Contribution of Authors

The authors declare that this work was done by the authors named in this article and all liabilities pertaining to claims relating to the content of this article will be borne by them.

Open Access

This is an Open Access article that uses a funding model which does not charge readers or their institutions for access and distributed under the terms of the Creative Commons Attribution License (<http://creativecommons.org/licenses/by/4.0>) and the Budapest Open Access Initiative (<http://www.budapestopenaccessinitiative.org/read>), which permit unrestricted use, distribution, and reproduction in any medium, provided the original work is properly credited.

REFERENCES

- Jonasch E, Gao J, Rathmell WK. Renal cell carcinoma. *Bmj-Brit Med J* 2014; 349: g4797.
- Xia R, Lin L, Yu S, Zhang J, Zheng L, Zhou L, Lin J. A systematic analysis of molecular mechanisms in non-metastatic renal cancer delineates affected regulatory pathways and genes in tumor growth. *Cell Mol Biol* 2021; 67(5): 427-438.
- Shao Y, Xiong S, Sun G, Dou W, Hu X, Yang W, Lia T, Deng S, Wei Q, Zeng H, et al. Prognostic analysis of postoperative clinically nonmetastatic renal cell carcinoma. *Cancer Med-Us* 2020; 9(3): 959-970.
- Li H, Qu L. Correlation of miRNA-21 and blood Cr levels with tumor infiltration and distant metastasis in renal cancer patients. *Cell Mol Biol* 2022; 68(5): 117-123.
- Barata PC, Rini BI. Treatment of renal cell carcinoma: Current status and future directions. *Ca-Cancer J Clin* 2017; 67(6): 507-524.

6. Dizman N, Adashek JJ, Hsu J, Bergerot PG, Bergerot CD, Pal SK. Adjuvant treatment in renal cell carcinoma. *Clin Adv Hematol Onc* 2018; 16(8): 555-563.
7. Makhov P, Joshi S, Ghatalia P, Kutikov A, Uzzo RG, Kolenko VM. Resistance to systemic therapies in clear cell renal cell carcinoma: Mechanisms and management Strategies. *Mol Cancer Ther* 2018; 17(7): 1355-1364.
8. Parekh H, Griswold J, Rini B. Axitinib for the treatment of metastatic renal cell carcinoma. *Future Oncol* 2016; 12(3): 303-311.
9. Roelants C, Pillet C, Franquet Q, Sarrazin C, Peilleron N, Giacosa S, Guyon L, Fontanell A, Fiard G, Long JA, et al. Ex-vivo treatment of tumor tissue slices as a predictive preclinical method to evaluate targeted therapies for patients with renal carcinoma. *Cancers* 2020; 12(1): 232.
10. Beetz O, Soffker R, Cammann S, Oldhafer F, Vondran F, Imkamp F, Klempnauer J, Kleine M. Extended hepatic metastasectomy for renal cell carcinoma-new aspects in times of targeted therapy: a single-center experience over three decades. *Langenbeck Arch Surg* 2020; 405(1): 97-106.
11. D'Aniello C, Berretta M, Cavaliere C, Rossetti S, Facchini BA, Iovane G, Mollo G, Capasso M, Pepa CD, Pesce L, et al. Biomarkers of Prognosis and Efficacy of Anti-angiogenic Therapy in Metastatic Clear Cell Renal Cancer. *Front Oncol* 2019; 9: 1400.
12. Chen X, Huang J, Peng Y, Han Y, Wang X, Tu C. The role of circRNA polyribonucleotide nucleoside transferase 1 on gestational diabetes mellitus. *Cell Mol Biol* 2022; 68(6): 148-154.
13. Li X, Wang T, Chen Q, Fu Q, Cui Y, Pan H. CircRTN4 inhibits the progression of gastric cancer by sponging miR-424-5p and regulating LATS2 expression. *Trop J Pharm Res* 2023; 22(5):967-974 doi: 10.4314/tjpr.v22i5.5
14. Feng Y, Wang W, Liu C. Effect of Solanum lyratum polysaccharide on malignant behaviors of lung cancer cells by regulating the Circ_UHRF1/miR-513b-5p Axis. *Cell Mol Biol* 2021; 67(6): 191-199.
15. Xiao MS, Ai Y, Wilusz JE. Biogenesis and functions of circular RNAs come into focus. *Trends Cell Biol* 2020; 30(3): 226-240.
16. Du WW, Zhang C, Yang W, Yong T, Awan FM, Yang BB. Identifying and Characterizing circRNA-Protein Interaction. *Theranostics* 2017; 7(17): 4183-4191.
17. Zhang Q, Wang W, Zhou Q, Chen C, Yuan W, Liu J, Li X, Sun Z. Roles of circRNAs in the tumour microenvironment. *Mol Cancer* 2020; 19(1): 14.
18. Verduci L, Strano S, Yarden Y, Blandino G. The circRNA-microRNA code: emerging implications for cancer diagnosis and treatment. *Mol Oncol* 2019; 13(4): 669-680.
19. Kristensen LS, Hansen TB, Venø MT, Kjems J. Circular RNAs in cancer: opportunities and challenges in the field. *Oncogene* 2018; 37(5): 555-565.
20. Yu Q, Liu P, Han G, Xue X, Ma D. CircRNA circPDSS1 promotes bladder cancer by down-regulating miR-16. *Bioscience Rep* 2020; 40(1): BSR20191961.
21. Ouyang Y, Li Y, Huang Y, Li X, Zhu Y, Long Y, Wang Y, Guo X, Gong K. CircRNA circPDSS1 promotes the gastric cancer progression by sponging miR-186-5p and modulating NEK2. *J Cell Physiol* 2019; 234(7): 10458-10469.
22. Stockhausen K. The Declaration of Helsinki: Revising ethical research guidelines for the 21st century. *Med J Aust* 2000; 172(6): 252-253.